Coupled Systems Mechanics, *Vol. 14, No. 3 (2025) 201-229*
https://doi.org/10.12989/csm.2025.14.3.201

Mathematical and finite element investigation on time period of coupled steel frames subjected to earthquake excitations

Omid Fereidooni[a], Panam Zarfam* and Mohammadreza Mansoori[b]

Department of Civil Engineering, Science and Research Branch, Islamic Azad University, Tehran, Iran

(Received June 5, 2024, Revised May 10, 2025, Accepted May 21, 2025)

Abstract. Current design codes of practice ignore the effect of interaction between primary and secondary systems when addressing the seismic response of coupled structures. The present investigation offers a robust mathematical representation of such interaction through a closed-form calculation of time periods in coupled primary-secondary systems. On this wise, an analytic framework was established to determine the fundamental period of a three-dimensional (3D) steel moment-resisting frame structures. The successful verification of the analytic formulation followed using a finite element (FE) modeling approach. Subsequently, a parametric study was carried out to address the effect of number and location of secondary systems, as well as number of frame stories, on the overall seismic response of the coupled system. The mass of secondary system was considered less than 20% of that of the primary system. Based on the FE modeling results, the most significant effect of secondary system on the response of coupled system relates to time period, which should be taken into account in current design procedures. Despite the very low mass of secondary system, time period of the coupled frame changed significantly, when the secondary system was added to primary structure. This causes the amplification of lateral drifts and deformations, leading to structural and non-structural damage, and potential failure. On the contrary, the fundamental period of short-rise frames increased with increasing secondary-to-coupled-system mass ratio. Based on this finding, it is viable to increase the time period of short-rise structures under the effect of secondary system period, and thus improve their seismic performance.

Keywords: coupled system; earthquake excitation; finite-element modeling (FEM); seismic response; steel frame; time period

1. Introduction

Many studies have explored the interaction between primary and secondary systems in coupled structures (Sari and Korkmaz 2024, Zhang *et al.* 2024, Lahdiri and Kadri 2024, Caicedo *et al.* 2021, Dhakal *et al.* 2016, Butenweg *et al.* 2021, Yang *et al.* 2022, Perrone *et al.* 2016). However, the computational complexity of these studies makes them impractical for use as design techniques. As a result, simplified methods for analyzing and designing coupled systems have been introduced (Ghafoori-Ashtiani and Foyooz 2022, Butenweg *et al.* 2021, Ryan *et al.* 2016).

*Corresponding author, Assistant Professor, E-mail: zarfam@srbiau.ac.ir
[a]Ph.D. Candidate
[b]Assistant Professor

http://www.techno-press.org/?journal=csm&subpage=8 ISSN: 2234-2184 (Print), 2234-2192 (Online)

Adam (2001) conducted experimental research focusing on the behavior of secondary systems, particularly when their frequency is close to that of the primary structure. Filiatrault *et al.* (2021) highlighted that the performance of coupled structures is often compromised due to damage or collapse of non-structural components, which is unacceptable for critical infrastructures. They advocated for more experimental research in this area. A straightforward floor response spectrum (FRS) method was later proposed to analyze the response of non-structural equipment (Merino *et al.* 2019, Surana 2019). This method estimates the maximum response of the secondary system using the response spectrum derived from the primary structure's response. Kazantzi *et al.* (2020) investigated strength reduction factors for designing lightweight non-structural elements and provided approximate equations for estimating system response. Chalarcal *et al.* (2020) examined the seismic demands on acceleration-sensitive non-structural components in braced frames.

Many studies have asserted that the fundamental period of a structure is the crucial parameter influencing its seismic behavior. Accurately determining this parameter is essential for predicting the structure's seismic response. In recent years, researchers have focused on developing precise methods to determine the fundamental period of various structures under different conditions (Zhao *et al.* 2020, Jiang *et al.* 2020a, b, De *et al.* 2018). It is now well-established that adding secondary systems alters the fundamental period of the primary structure. However, the impact of this change on the primary structure's period has not been adequately addressed in previous research, leading to limited studies on the period of structures (Asteris *et al.* 2017, Charalampakis *et al.* 2020). Overlooking this aspect can result in computational inaccuracies when predicting the seismic behavior of secondary and coupled structures. Pandian and Vinu (2023) have comprehensively examined the effects of fundamental periods on the seismic performance of base-isolated multi-story buildings.

Reviewing the current literature shows that secondary systems have often been viewed as detrimental and threatening to structural safety. Consequently, their seismic behavior has been a priority in recent studies. However, due to the complexity of primary-secondary system interactions (PSSI), design techniques have typically relied on simplified assumptions. The most common approach has been to ignore PSSI and assume that the secondary and primary systems behave independently. This assumption is prevalent in seismic codes, where the secondary system is treated as a single, independent system with a small mass. As a result, the multiplicity of secondary systems and their collective significant mass have not been thoroughly addressed, as PSSI is often disregarded. However, the presence of multiple secondary systems and their total mass can influence the seismic behavior of the structure. One benefit is the potential increase in the period of the coupled system, which can improve seismic behavior by reducing the structure's base acceleration. Despite this, there is a lack of simple, practical methods for calculating the fundamental period of a coupled system. Therefore, efforts have focused on creating conditions where primary and secondary structures do not interfere, often neglecting the effects of secondary systems on the coupled structure's seismic behavior. Additionally, structural engineers may overlook interaction effects due to the relatively small mass of individual secondary systems compared to the primary structure, leading to uncertainty about changes in the primary structure's behavior when influenced by secondary systems.

1.1 Significance of study

Until now, technical literature has primarily considered period or frequency as secondary parameters in calculating system response or the equation of motion. These parameters have often

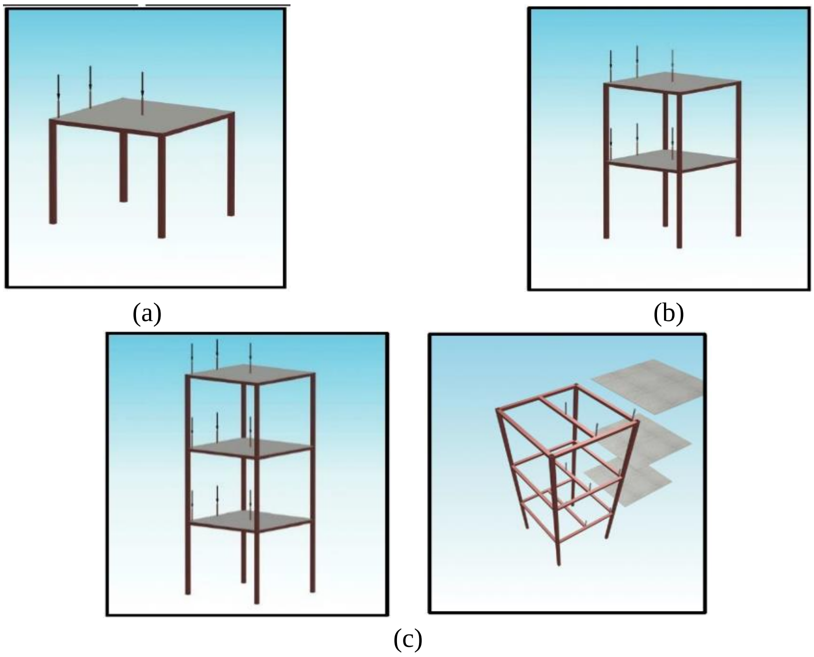

Fig. 1 FE model of (a) one-story, (b) two-story, and (c) three-story coupled structures with the corresponding loadings

been overlooked because the response of secondary and primary systems is typically assumed to be independent, given the negligible mass of the secondary system compared to the primary system. However, this study emphasizes the impact of the secondary system on the response of the coupled system during the design process, with the most significant effect being on the period. Due to the presence of multiple secondary systems, their total mass cannot be disregarded in calculations. Moreover, the proposed approach offers the benefit of adjusting the period of primary structures with shorter periods, allowing the coupled structure to take advantage of increased period values through the use of multiple secondary systems. This adjustment can enhance the overall seismic performance of the structure.

2. Mathematical formulation

A set of three-dimensional (3D) moment-resisting frame structures with one, two, and three stories were chosen as primary systems. Each structure features four perimeter columns and four perimeter beams at each story, as depicted in Fig. 1. The detailed specifications of these selected frames are discussed in “Section 3. Finite Element Modeling”.

The authors’ preliminary findings indicated that the most critical factor in determining the response of coupled systems is the period of these systems relative to the fundamental period of the primary structure. Knowing the period of the coupled system allows for characterizing its behavior. Therefore, in this section, the dynamic relationships of coupled systems were examined to develop a mathematical representation that can estimate the period of the coupled system with an acceptable degree of accuracy. Initially, general relationships were established for the secondary system. Subsequently, a simplified relationship was proposed as a design technique for estimating the period of the coupled system. This simplified relationship is based on a series of simplifying assumptions. To calculate the fundamental period of the coupled system, the mass and stiffness matrices must be established, followed by the computation of the characteristic equation. Other researchers have undertaken this process for a single secondary system. Here, a similar approach will be extended to accommodate multiple and more complex secondary systems. It is important to note the following indexing conventions:

- Index *p* denotes characteristics of the primary system.
- Index *s* denotes characteristics of the secondary systems.
- Index *c* denotes characteristics of the coupled system.
- Index *i* indicates the degree of freedom (DOF) of the primary system.
- Index *j* indicates the DOF of the secondary system.

Mass and stiffness of each single-degree-of-freedom (SDOF) secondary system are given by $m_{s\,ij}$ and $k_{s\,ij}$ respectively, representing the mass and stiffness of the *j*-th secondary system attached to the *i*-th DOF of the primary system. Suppose there are *m* SDOF secondary systems connected to various DOFs of the primary system, which has *n* DOFs. The mass and stiffness matrices of the primary system are represented by $[M_p]$ and $[K_p]$, while those of the coupled system are represented by $[M_c]$ and $[K_c]$.

$$[M_c] = \begin{bmatrix} [M_{pp}]_{n*n} & [M_{ps}]_{n*m} \\ [M_{sp}]_{m*n} & [M_{ss}]_{m*m} \end{bmatrix}$$
$$[K_c] = \begin{bmatrix} [K_{pp}]_{n*n} & [K_{ps}]_{n*m} \\ [K_{sp}]_{m*n} & [K_{ss}]_{m*m} \end{bmatrix} \tag{1}$$

in which $[M_{pp}]_{n*n}$ represents primary system mass matrix with *n* DOFs, $[M_{ps}]_{n*m}$ and $[M_{sp}]_{m*n}$ are zero matrices, $[M_{ss}]_{m*m}$ shows secondary system mass matrix with count *m*, which is a diagonal matrix with each member equal to mass of the corresponding secondary system, $[K_{pp}]_{n*n}$ is primary system stiffness matrix, members in $[K_{ps}]_{n*m}$ are negative of corresponding secondary system stiffness, $[K_{sp}]_{m*n}$ is transpose of $[K_{ps}]_{n*m}$, and $[K_{ss}]_{m*m}$ denotes diagonal secondary system stiffness matrix. These terms have expressed by mathematical terms in Eq. (2).

$$[M_{pp}] = [M_p]$$
$$[M_{ps}] = [M_{sp}] = 0$$
$$\begin{cases} M_{ss\ \ a.a} = m_{sj} & if\ \ a = j \\ M_{ss\ \ a.b} = 0 & if\ \ a \neq b \end{cases}$$
$$[K_{pp}] = [K] + [K_s]$$
$$\begin{cases} K_{s\ \ a.a} = k_{sj} & if\ \ a = i \\ K_{s\ \ a.b} = 0 & if\ \ a \neq i \end{cases}$$
$$K_{pp\,ai} = k_{p\,ai}\ \ \&\ \ \ K_{pp\,ia} = k_{p\,ia}\ (if\ a \neq i)$$
$$\begin{cases} K_{ps\ \ a.b} = -k_{sj} & if\ \ a = i\ \&\ \ b = j \\ K_{ps\ \ a.b} = 0 & if\ \ a \neq i\ \ OR\ \ b \neq j \\ [K_{ps}] = [K_{sp}]^T \end{cases}$$

$$\begin{cases} K_{ss\ \ a.a} = k_{sj} & if\ \ a = j \\ K_{ss\ \ a.b} = 0 & if\ \ a \neq b \end{cases} \tag{2}$$

To calculate the period of a coupled system, one must calculate the characteristic equation (Eq. (3)) and obtain its determinant.

$$|[K_c] - {\omega_c}^2[M_c]| = 0 \tag{3}$$

in which ω_c is the natural frequency of the coupled system. Given that we assumed the primary system has n DOFs, to which m secondary systems are attached, the *j*-th mode shape of the coupled system can be expressed as Eq. (4)

$$\{\varphi_j^*\} = \begin{Bmatrix} \varphi_{1j}^* \\ \varphi_{2j}^* \\ \vdots \\ \varphi_{ij}^* \\ \vdots \\ \varphi_{nj}^* \\ \varphi_{n+1j}^* \\ \varphi_{n+2j}^* \\ \vdots \\ \varphi_{n+mj}^* \end{Bmatrix} \tag{4}$$

Assuming free vibration, the equation of motion in mode shape *r* of the coupled system reads

$$[K_c]\{\varphi_r^*\} = \omega_{cr}^2[K_c]\{\varphi_r^*\} \tag{5}$$

in which $\{\varphi_r{}^*\}$ is the modal vector in mode shape *r* with (*n*+*m*) rows. The *n* rows of Eq. (5) in mode shape *r* are as follows

$$[K]\begin{Bmatrix} \varphi_{1r}^* \\ \varphi_{2r}^* \\ \vdots \\ \varphi_{nr}^* \end{Bmatrix} + \{k_s\varphi^*\} = \omega_{cr}^2[M]\begin{Bmatrix} \varphi_{1r}^* \\ \varphi_{2r}^* \\ \vdots \\ \varphi_{nr}^* \end{Bmatrix} \tag{6}$$

Eq. (6) conveniently represents the motion equation of the coupled system in terms of primary and secondary systems. For example, if *m* secondary systems are attached to a primary system with four DOFs, assuming that the first secondary system is connected to second DOF in primary system, the second secondary system to fourth DOF, and the *m*-th secondary system to (*n*-1)-th DOF, then mode shape *r* reads

$$\{k_s\varphi^*\} = \begin{Bmatrix} 0 \\ k_{s1}(\varphi_{2r}^* - \varphi_{n+1r}^*) \\ 0 \\ k_{s2}(\varphi_{4r}^* - \varphi_{n+1r}^*) \\ \vdots \\ k_{sm}(\varphi_{n-1r}^* - \varphi_{n+1r}^*) \\ 0 \end{Bmatrix} \tag{7}$$

while the rest of the *m* rows can be expressed as

$$\begin{gathered}
-k_{s1}\left(\varphi_{ij}^{*}-\varphi_{n+1j}^{*}\right)=m_{s1}\omega_{cj}^{2}\varphi_{n+1j}^{*}\\
-k_{s2}\left(\varphi_{ij}^{*}-\varphi_{n+2j}^{*}\right)=m_{s2}\omega_{cj}^{2}\varphi_{n+2j}^{*}\\
\vdots\\
-k_{sm}\left(\varphi_{ij}^{*}-\varphi_{n+mj}^{*}\right)=m_{sm}\omega_{cj}^{2}\varphi_{n+mj}^{*}
\end{gathered} \tag{8}$$

in which index "i" is the DOF in primary system to which the secondary system is attached. Assuming that $k_s = m_s\omega_s^{*2}$, then Eq. (8) converts to Eq. (9)

$$\begin{gathered}
\varphi_{n+1j}^{*}=\frac{\omega_{s1}^{2}}{\omega_{cj}^{2}-\omega_{s1}^{2}}\varphi_{ij}^{*}\\
\varphi_{n+2j}^{*}=\frac{\omega_{s2}^{2}}{\omega_{cj}^{2}-\omega_{s2}^{2}}\varphi_{ij}^{*}\\
\vdots\\
\varphi_{n+mj}^{*}=\frac{\omega_{sm}^{2}}{\omega_{cj}^{2}-\omega_{sm}^{2}}\varphi_{ij}^{*}
\end{gathered} \tag{9}$$

The vector $\{ks\varphi^*\}$ in Eq. (6) with n rows, reflects the interaction of the secondary system on the primary system characteristic equation. If the j-th secondary system is attached to the i-th DOF, the i-th member of this vector in shape mode r equals $k_{sj}(\varphi_{ir}{}^{*}-\varphi_{n+1r}{}^{*})$, and the rest of the members are zero. Thus, assuming that j-th secondary system is connected to the i-th DOF, the i-th member of the vector $\{k_s\varphi^*\}$ in shape mode r reads

$$\{k_s\varphi^*\}_{ir}=\frac{m_{sj}\varphi_{ir}^{*}\omega_{cr}^{2}\omega_{sj}^{2}}{\omega_{cr}^{2}-\omega_{sj}^{2}} \tag{10}$$

The characteristic equation for the example of a primary system with four DOFs can be written as

$$[K]\begin{Bmatrix}\varphi_{1j}^{*}\\ \varphi_{2j}^{*}\\ \vdots\\ \varphi_{ij}^{*}\\ \vdots\\ \varphi_{nj}^{*}\end{Bmatrix}+\begin{Bmatrix}0\\ \frac{m_{s1}\varphi_{2j}^{*}\omega_{cj}^{2}\omega_{s1}^{2}}{\omega_{cj}^{2}-\omega_{s1}^{2}}\\ 0\\ \frac{m_{s2}\varphi_{4j}^{*}\omega_{cj}^{2}\omega_{s2}^{2}}{\omega_{cj}^{2}-\omega_{s2}^{2}}\\ \vdots\\ \frac{m_{sm}\varphi_{n-1j}^{*}\omega_{cj}^{2}\omega_{sm}^{2}}{\omega_{cj}^{2}-\omega_{sm}^{2}}\\ 0\end{Bmatrix}=\omega_{cj}^{2}[M]\begin{Bmatrix}\varphi_{1j}^{*}\\ \varphi_{2j}^{*}\\ \vdots\\ \varphi_{ij}^{*}\\ \vdots\\ \varphi_{nj}^{*}\end{Bmatrix} \tag{11}$$

The result in Eq. (10) can be neglected given that mass of the secondary system is small compared to the primary system, except for when the frequency of the secondary system is close to the frequency of the primary structure (i.e., resonance). Otherwise, by multiplying both sides of Eq. (11) by $\{\varphi_j\}^T$, it reads:

$$\omega_j^2 M_j+\sum_{r=1}^{m} m_{sr}\varphi_{ij}^{2}\frac{\omega_{cj}^{2}\omega_{sr}^{2}}{\omega_{cj}^{2}-\omega_{sr}^{2}}=\omega_{cj}^{2}M_j \tag{12}$$

in which ω_j is the frequency in *j*-th mode of primary system, M_j is the primary system mass matrix, m_{sr} the *r*-th secondary system mass, ω_{cj} the frequency of coupled system in *j*-th mode, and ω_{sr} is the frequency of *r*-th secondary system.

According to Rayleigh's hypothesis, a first-order error in mode shapes causes a second-order error in frequencies. As a matter of this fact, approximation of the first mode shape of primary and coupled systems will cause a negligible error in the estimation of frequency and time period. Therefore, given the importance of the first mode shape, one can simplify Eq. (12) only to the first mode, expressed by Eq. (13)

$$\omega_p^2 M_1 + \sum_{r=1}^{m} m_{sr}\varphi_{r1}^2 \frac{\omega_c^2\omega_{sr}^2}{\omega_c^2 - \omega_{sr}^2} = \omega_c^2 M_1 \tag{13}$$

in which ω_p represents the primary system frequency at first mode, M_1 the primary system mass contributing to the first mode, and ω_p denotes the coupled system frequency at first mode.

Although all secondary systems' frequencies cannot be presumed equal, yet the average of all frequencies can be implemented in order to solve the equation of motion for all secondary systems. Therefore, it is assumed that all the different frequencies of secondary systems can be equated with an effective frequency (ω_{se}). Replacing the term ω_{sr} in Eq. (13) by a constant value ω_{se} and dividing both sides of Eq. (13) by $\omega_p^4 M_1$, one can write

$$\left(\frac{\omega_c}{\omega_p}\right)^4 - \left(\frac{\omega_c}{\omega_p}\right)^2\left(\frac{\omega_s}{\omega_p}\right)^2\left(1+\frac{\sum m_{sr}\varphi_{r1}^2}{M_1}\right) + \left(\frac{\omega_s}{\omega_p}\right)^2 - \left(\frac{\omega_c}{\omega_p}\right)^2 = 0 \tag{14}$$

Here, we define the following parameters as frequency ratios

$$\begin{aligned} R_F &= \omega_c/\omega_p \\ r_F &= \omega_s/\omega_p \end{aligned} \tag{15}$$

By replacing the terms in Eq. (15) into Eq. (14), and by knowing that $M_1 = \{\varphi_1\}^{\mathrm{T}}[M]\{\varphi_1\} = \sum_{i=1}^{n} m_i\varphi_{i1}^2$, it reads

$$R_F^4 - \left(1 + r_F^2 + \frac{\sum_{r=1}^{n}(m_{sr}\varphi_{r1}^2)}{\sum_{i=1}^{n}(m_i\varphi_{i1}^2)} r_F^2\right) R_F^2 + r_F^2 = 0 \tag{16}$$

According to dynamic analysis of structures, shape mode functions of regular structures can be expressed as sine functions. Thus, by extending the power series of these sine functions and disregarding the terms except for the first term, the first mode shape will be a simple linear function, expressed by Eq. (17)

$$\varphi_{ij} = sin\left(\frac{2j-1}{2n+1} i\pi\right) \approx \frac{\pi}{2n+1} m \quad (m = 1.2 \ldots .n) \;\Rightarrow\; \varphi_{i1} \approx h_i \tag{17}$$

By defining $\gamma = \frac{\sum_{r=1}^{n}(m_{sr}\varphi_{r1}^2)}{\sum_{i=1}^{n}(m_i\varphi_{i1}^2)}$ as the mass ratio and inserting Eq. (16) into Eq. (16), it reads

$$R_F^4 - (1 + r_F^2 + \gamma r_F^2) R_F^2 + r_F^2 = 0 \qquad \left(\gamma = \frac{\sum(m_s h_s^2)}{\sum(m_p h_p^2)}\right) \tag{18}$$

Eq. (18) is the solution to the characteristic relation of the coupled system. However, since it is

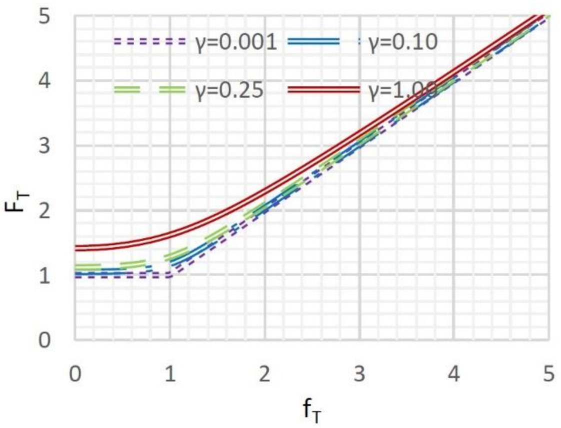

Fig. 2 Variations of F_T versus f_T in terms of different mass ratios

customary to express this relation in terms of time period in design techniques, especially seismic calculations. Therefore, Eq. (14) can be expressed in terms of time period shown by Eq. (19)

$$\frac{{T_p}^4}{{T_c}^4}-\left(\frac{{T_p}^4}{{T_c}^2{T_{se}}^2}\right)\left(1+\frac{\sum m_{sr}\varphi_{r1}^2}{M_1}\right)+\frac{{T_p}^2}{{T_{se}}^2}-\frac{{T_p}^2}{{T_c}^2}=0 \tag{19}$$

in which T_p is primary system period, T_c the coupled system period, and T_{se} represents the effective time period of the secondary systems. Here we define the following parameters as time and mass ratios

$$\begin{gathered} F_T=\frac{1}{R_F}=\frac{T_c}{T_p} \\ f_T=\frac{1}{r_F}=\frac{T_s}{T_p} \\ \acute{\gamma}=1+\frac{\sum(m_s h_s^2)}{\sum(m_p h_p^2)} \end{gathered} \tag{20}$$

where, F_T is the ratio of the coupled system period to the primary system period, f_T is the ratio of the secondary system period to the primary system period, and γ is the mass correction ratio. It is observed that this relationship is similar to the coupled system with a secondary system relationship, with the difference that the definitions of mass ratio and secondary system period have been changed in this relationship and have been defined for the multiplicity of secondary systems more comprehensively. Thus, Eq. (14) can be expressed as

$${F_T}^4-\left({f_T}^2+\acute{\gamma}\right){F_T}^2+{f_T}^2=0 \tag{21}$$

To derive Eq. (21), it was initially assumed that all varying periods of the secondary systems could be represented by a single effective period. Consequently, the values of T_{se} and γ must be determined to capture the collective effects of all secondary systems. The influence of each of these parameters on the period of the coupled system needs to be examined. While in some specialized structures the mass of the secondary system might exceed that of the primary system, in conventional building structures, the mass of the secondary systems is typically less than that of

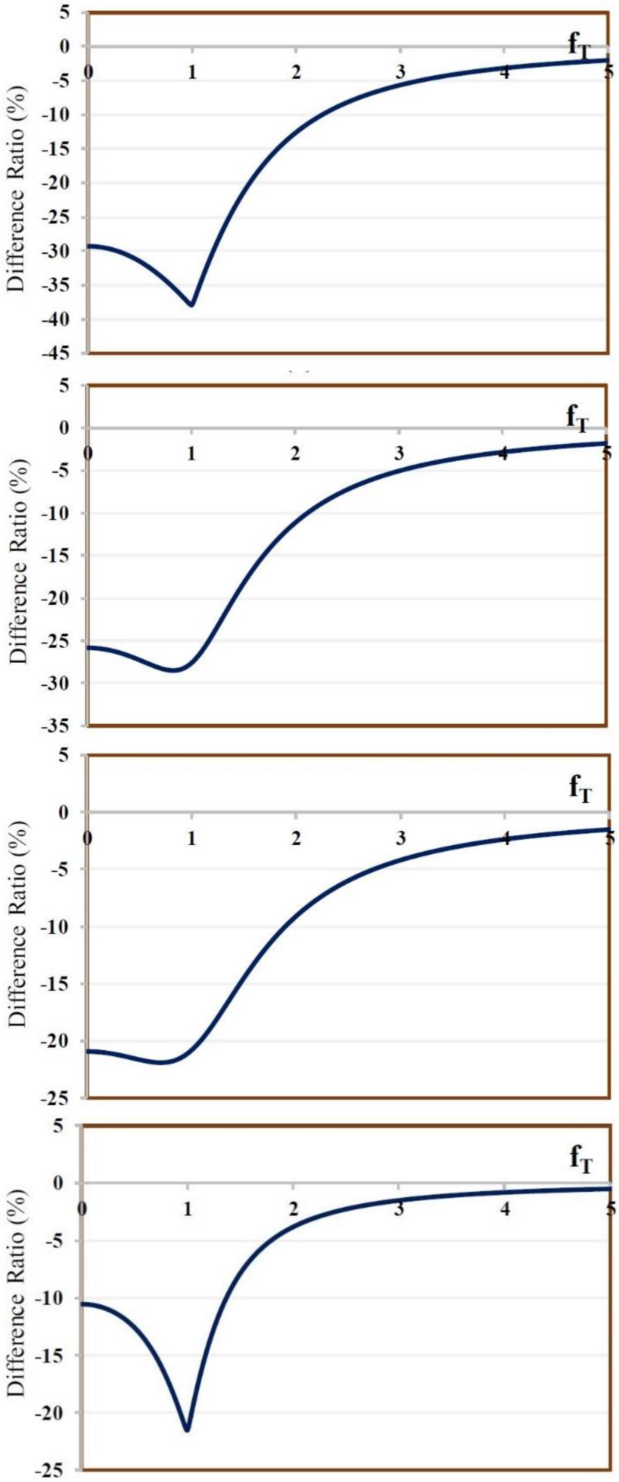

Fig. 3 Variations of F_T against different mass ratios at (a) γ=0.001 compared to γ =1.00; (b) γ=0.1 compared to γ=1.00; (c) γ=0.25 compared to γ=1.00; (d) γ=0.001 compared to γ =0.25

the primary system. Therefore, in conventional buildings, it can be assumed that γ falls between zero and one. To better understand the impact of γ on the period of the coupled system, the values of F_T were calculated against f_T for five different ratios of γ: 0.0001, 0.01, 0.10, 0.25, and 1.00, as illustrated in Fig. 2.

By examining the diagram in Fig. 2, it is clear that F_T values do not increase much up to f_T=1. However, after that, the coupled system period increases more and the relationship of F_T and f_T tends to be linear. Besides, with increasing f_T, the difference between diagrams with different mass ratios decreases. This is indicative of the fact that with increasing f_T the effect of mass ratio on the coupled system period is decreased. To better understand the context, the F_T changes at different γ values were estimated in comparison with F_T at γ=1.00 and 0.25, as shown in Fig. 3.

Fig. 3 shows that the effect of mass ratio on the period of coupled systems has an increasing trend until f_T reaches 1. But after that, the effect of mass ratio decreases with increasing f_T, so that after f_T=3, the F_T change between different mass ratios is less than 5%. The major change of F_T is observed between the two states of γ=0.0001 and γ=1.00 at f_T= 1, which has a value of less than 40%. It can be concluded that the main factor in determining the period of a coupled system is f_T, and the effect of γ is much less than f_T. Also, as the value of f_T becomes larger than 1, the effect of γ on F_T decreases. Therefore, it can be assumed that the coupled system period is affected by the period of any of secondary systems connected to the primary structure, which, if considered alone, will have the greatest effect on the coupled system period compared to other secondary systems. Due to the lower effects of the other secondary systems period, they can change the primary system period as a secondary mass. To identify the effective secondary period, it is suggested that each of the secondary systems be added to the primary system and the F_T value be calculated for each separately using Eq. (21). The secondary system with a maximum F_T will then be selected as the effective secondary system, and its period can be chosen as T_{se}. The other secondary system periods will not affect the coupled system period, but their mass must be added to the mass ratio, so that it appears different from the mass of the effective secondary system. According to Fig. 3, if f_{Te}≥3, one can ignore the mass effect of other secondary systems with a reasonable margin of error. For f_{Te}<3, the equivalent secondary mass for inefficient secondary systems need to be calculated. Writing Eq. (21) for the defined mass ratio gives

$$\gamma = \frac{{F_T}^4 + {f_T}^2}{{F_T}^2} - \left({f_T}^2 + 1\right) \tag{22}$$

To better examine the time periods of different coupled systems with different secondary systems, let's assume that two different secondary systems are attached to a primary system, such that n secondary systems of the first type with period and mass ratios of f_{T1} and γ_1, and m secondary systems of the second type with period and mass ratios of f_{T2} and γ_2. Let's also assume $f_{T1} > f_{T2}$. Now if $\gamma_1 \geq \gamma_2$, then the effective period of the secondary systems will definitely be f_{T1} and the second type secondary systems contribute only through their mass. However, if $\gamma_1 < \gamma_2$, each of the secondary systems can be chosen as an effective secondary system in the estimation of the coupled system period. In either case, time periods of the coupled system are T_{C1} and T_{C2}. Thus, larger period indicates the greater effect of that secondary system, and that period can be considered as the effective time period (f_{Te}) for the coupled system. In order to obtain an equivalent secondary system with a similar time period as another secondary system, given that both systems have similar effects, Eq. (22) gives two distinct mass ratios γ_i=1,2, as expressed by Eq. (23)

Table 1 Specifications of input ground motion records

ID No.	Earthquake			Recording Station	Record Seq. No.	Lowest Freq (Hz.)	PGA (g)	PGv (cm/sec)
	M	Year	Name					
1	6.7	1994	Northridge	Beverly Hills-Mulhol	953	0.25	0.52	**63**
2	7.1	1999	Duzce,Turkey	Bolu	1602	0.06	0.82	**62**
3	6.9	1995	Kobe,Japan	Nishi-Akashi	1111	0.13	0.51	**37**
4	7.3	1992	Landers	Coolwater	848	0.13	0.42	**42**
5	6.9	1989	Loma Prieta	Capitola	752	0.13	0.53	**35**
6	7.4	1990	Manjil,Iran	Abbar	1633	0.13	0.51	**54**
7	7.6	1999	Chi-Chi,Taiwan	TCU045	1485	0.05	0.51	**39**

Table 2 Scale factors for the ground motion excitations in the preliminary analysis step

ID No.	Earthquake	Scaling Factor
1	Northridge	**0.7941**
2	Duzce, Turkey	**1.0405**
3	Kobe, Japan	**0.6996**
4	Landers	**0.6406**
5	Loma Prieta	**0.6509**
6	Manjil, Iran	**1.0971**
7	Chi-Chi, Taiwan	**1.0171**

$$\gamma_i{}^* = \gamma_i - \left(f_{Te}{}^2 - f_{Ti}{}^2\right)\left(1 - \frac{1}{F_{Ti}{}^2}\right) \tag{23}$$

The value of F_T is always larger than 1. Therefore, two cases can be investigated:

(1) if $f_{Te} > f_{Ti}$, the second part of Eq. (23) becomes negative, and as a result $\gamma_i^* < \gamma_i$. Accordingly, considering the lower effect of mass ratio as compared to time period, the result will be achieved with a simplifying assumption. However, if the period of a secondary system in a coupled system is smaller than the effective secondary period, its period and mass effects can be completely disregarded,

(2) if $f_{Te} \leq f_{Ti}$, the mass ratio of the not-effective secondary system has to be included in the calculations using Eq. (23). Meanwhile, considering the lower effect of mass ratio compared to period, it is assumed that γ_i^* is equal to γ_i through another simplifying assumption. In other words, if the secondary system period in a coupled system is greater than the effective secondary period, its period effect can be neglected, and only its mass ratio is added to the mass ratio of the effective secondary system. Therefore, Eq. (24) can be established in the calculation of the time period of the coupled system. In a generalized form, if *r* types of secondary systems, each consisting of *m* similar systems with time period T_{sr} and weight w_{sr}, are connected to an *n*-DOF primary system with time period T_p and story weight w_p, then the effective period of the coupled system for each secondary system is expressed by Eq. (24).

$$T_c{}^2 = \frac{T_p{}^2}{2}\left(\alpha + \sqrt{\alpha^2 - 4f_T{}^2}\right)$$
$$\alpha = f_T{}^2 + \gamma_e{}^* + 1 \quad \& \quad f_T{}^2 = \frac{T_{se}{}^2}{T_p{}^2} \tag{24}$$

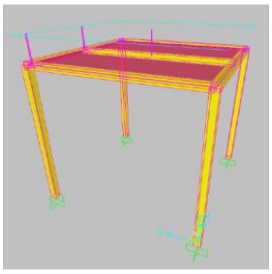

(a)

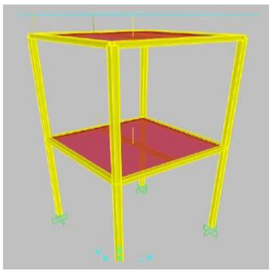

(b)

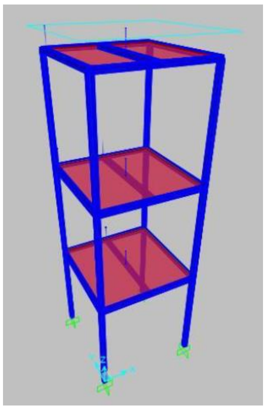

(c)

Fig. 4 FE model of (a) one-story, (b) two-story, and (c) three-story coupled frame structures

3. Finite element modeling

A number of three-dimensional (3D) moment-resisting frame structures with one, two, and three stories, each featuring four perimeter columns and four perimeter beams per story, were modeled using a finite element method (FEM) software (Alami and Khotimah 2017) as primary systems (Fig. 1). In these models, columns and beams were made of box sections with dimensions 150×150 mm. Additionally, each floor was represented by a 5-mm thick steel plate with material properties matching those of the other steel components. The height of each story along the vertical axis was 4500 mm, and the spans along both horizontal axes were also 4500 mm.

Reinforcing bars with lengths of 400 mm and diameters of 6 mm were attached to the primary system to model the secondary systems, which had a total mass of less than 20% of the primary system's mass. Fig. 4 shows schematic of the FEM of the one-, two-, and three-story coupled structures with the corresponding loadings. The moment frames act as primary systems, the attached rebars act as secondary systems, and the entire structure acts as a coupled system.

In order to perform the finite element analysis, a total of seven ground motion records obtained from PEER-NGA were selected and scaled in accordance with ASCE7-16 recommendations so as to represent a wide range of amplitudes (Tables 1 and 2).

It is notable that the weight of each individual secondary system was only 0.3% of the primary system's weight, making it relatively insignificant. The reinforcing bar (rebar) models were tied to the frame floor at various locations on each floor, with different configurations but similar stiffness and seismic specifications.

As regards to the selection of records, it should be heeded that Moeindarbary and Taghikhani (2014) confirmed that the optimal design variables in three levels of service level earthquake (SLE), design basis earthquake (DBE), and maximum considered earthquake (MCE) are close in characteristics, and hence, hazard levels play no significant role in the selection procedure. As part of the analysis step, a non-linear dynamic time-history analysis was carried out. Then, to compare the seismic response of the coupled system period with that obtained from the analytic approach, diagrams demonstrating the percentage of difference between the associated responses were plotted versus variations in the mass ratio (ɣ). The steel material was considered ordinary structural steel with elastic modulus of 200 GPa, yield stress of 240 MPa, and Poisson's ratio of 0.3. Also, a bi-linear model featuring strain hardening capacity was applied to simulate the nonlinear and inelastic properties of the steel material. As such, the plastic strain varied from the yield strain of 0.6 to the ultimate strain. The wall material was modeled as brick tiles with an elastic modulus of 1448 MPa, compressive strength of 2.5 MPa, and Poisson's ratio of 0.3. Concrete Damage Plasticity (CDP) feature was adopted to model the fracture behavior of the bricks.

All the modeled primary and coupled frame structures were first analyzed using modal analysis, and their fundamental periods were precisely calculated using the FE software. The period of the coupled system was then determined using Eq. (24). The discrepancy between the proposed relationship for the coupled structural period and the results from numerical analysis was also assessed. Due to the complexity of the dynamic interactions between primary and secondary systems, previous studies serving as the basis for design code relationships have often overlooked these interaction effects. Instead, secondary systems have been treated merely as additional mass on the primary structure. In the numerical part of this study, an effort was made to develop a simple design technique for calculating the fundamental period of a coupled system, considering the multiplicity of secondary systems. This involved building upon previous research and simplifying the dynamic relationships. Consequently, the fundamental period of the coupled structure is used in place of the primary structure's period in seismic design relationships and techniques.

4. Results and discussion

The periods associated with coupled systems, formed by combining a SDOF primary system with one, two, ten, and twenty secondary systems, are calculated based on results from both FEM and the proposed mathematical relationship (Eq. (24)). The periods of the modeled frame structures, as obtained from FE software, are presented in Figs. 5 to 8. The secondary systems were modeled with varying stiffness values, labeled as SS1 to SS5 in the figure legends. The stiffness of the secondary systems increases from SS1 to SS5. Based on the results in Fig. 5, the time period of a one-story frame structure coupled with a single secondary system increases with the mass ratio (γ) in both FE and mathematical approaches. The trends shown in the two diagrams (Fig. 5 (a) and (b)) are nearly identical for both methodologies. It is also evident that increasing the stiffness of the secondary system reduces the period of the coupled primary-secondary structure. Additionally, the difference ratio between the numerical and proposed analytical methods is illustrated in Fig. 5(c). This figure shows that the difference ratio ($T_{c-mathematical}/T_{c-FEM} - 1$) generally increases with the mass ratio (γ). The discrepancy is smallest when the stiffness of the

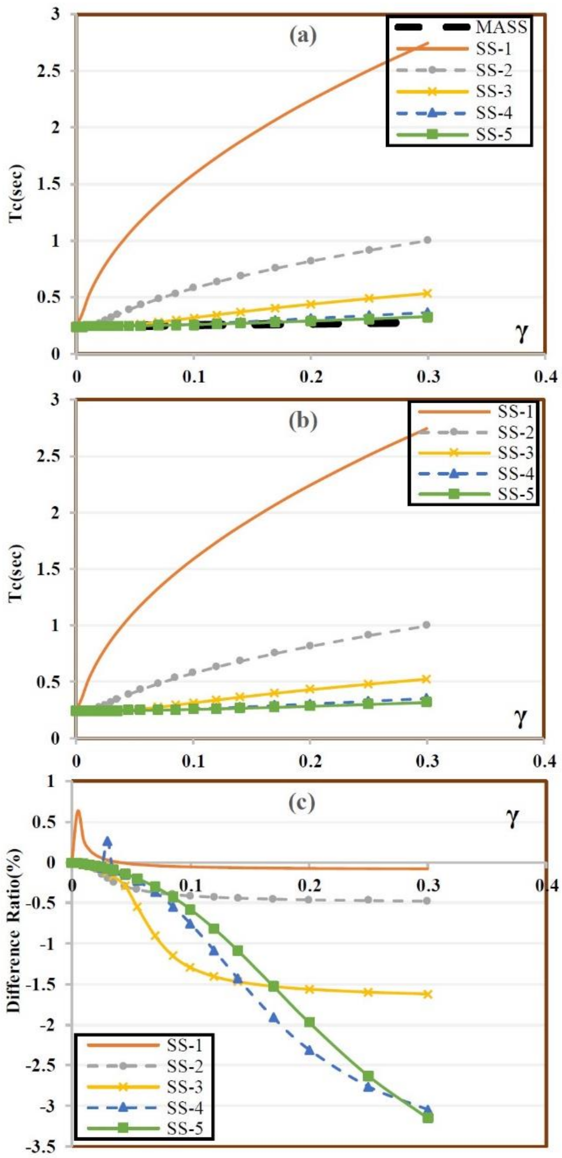

Fig. 5 Changes in time periods of one-story frame coupled with one secondary system against mass ratio (γ): (a) FEM, (b) proposed Eq. (24), and (c) difference ratio ($T_{c-mathematical}/T_{c-FEM} - 1$)

secondary system is at its lowest. Therefore, the period ratio increases as the stiffness of the secondary system is elevated.

The time periods of a one-story frame structure coupled with two secondary systems are shown against the mass ratio (γ) for various secondary system stiffness values in Fig. 6. Both FE and mathematical approaches exhibit a similar trend in the variation of the coupled system periods. In both methods, the period of the coupled system increases with a higher mass ratio. Additionally, an increase in the stiffness of the secondary system results in a decrease in the period of the

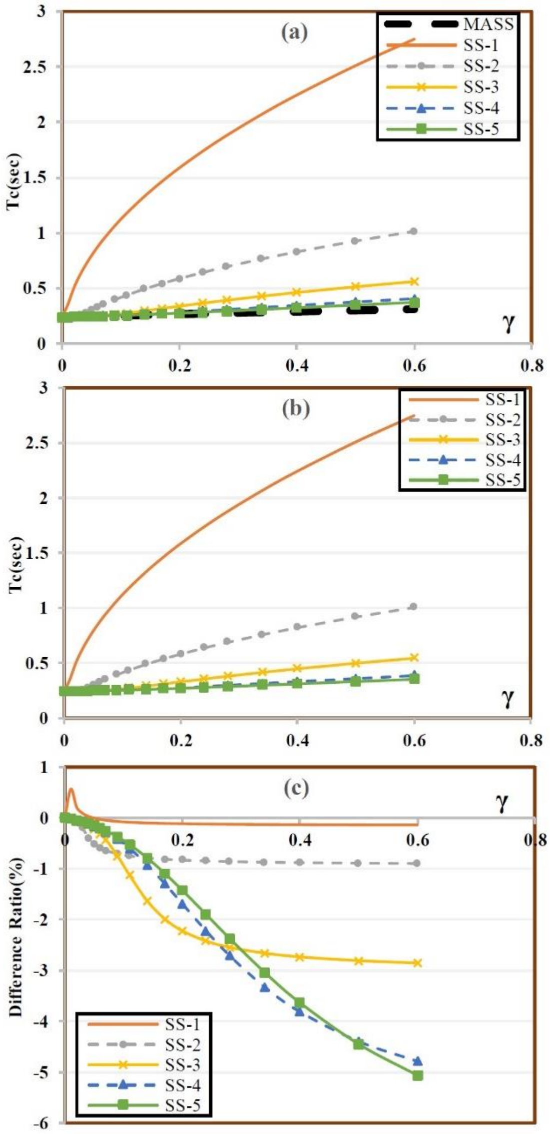

Fig. 6 Changes in time periods of one-story frame coupled with two secondary systems against mass ratio (γ): (a) FEM, (b) proposed Eq. (24), and (c) difference ratio ($T_{c-mathematical}/T_{c-FEM} - 1$)

coupled system.

Similarly, Fig. 7 displays the fundamental period of a single-story frame structure coupled with ten secondary systems against various mass ratios (γ). According to the figure, the longest period is observed when the secondary system has the lowest stiffness, i.e., SS1. Thus, in both methods, the period of the coupled system decreases as the stiffness of the secondary system increases. Moreover, the difference in the system period between the two approaches is smallest for systems with the lowest secondary system stiffness.

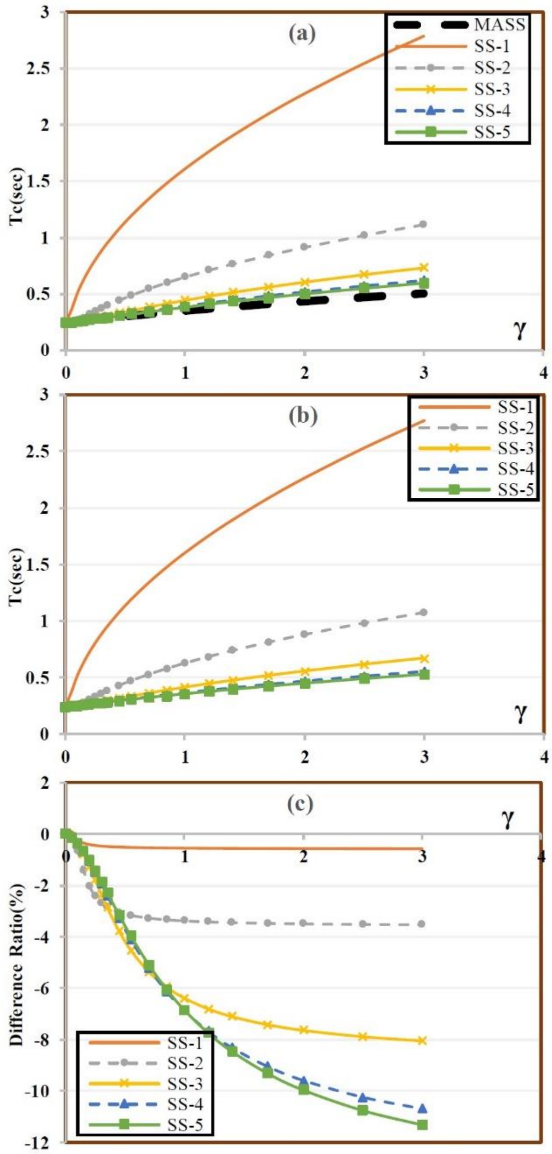

Fig. 7 Changes in time periods of one-story frame coupled with ten secondary system against mass ratio (γ): (a) FEM, (b) proposed Eq. (24), and (c) difference ratio ($T_{c-mathematical}/T_{c-FEM}-1$)

The time period of a single-story frame structure coupled with twenty secondary systems is plotted against various mass ratios (γ) in Fig. 8. It is observed that the same trend in period variation holds true for systems with twenty secondary systems of different stiffnesses, similar to those with fewer secondary systems. However, Fig. 8 also shows that the period discrepancy between the two approaches increases as the number of secondary systems grows.

Examining the diagrams reveals that for single-story coupled frame structures with a low number of secondary systems, the difference between the results from the proposed Eq. (24) and

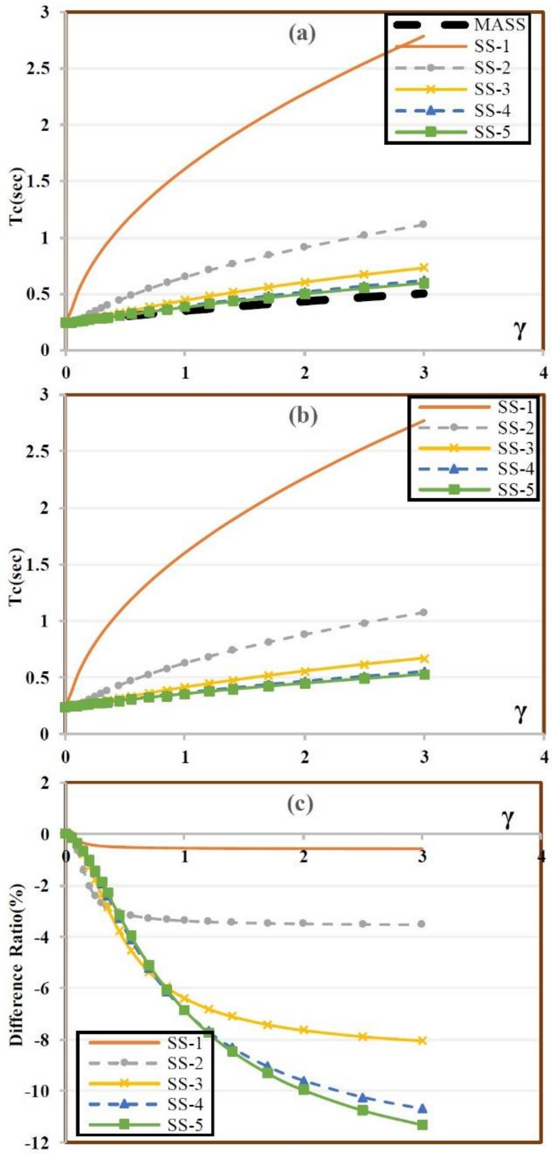

Fig. 7 Changes in time periods of one-story frame coupled with ten secondary system against mass ratio (γ): (a) FEM, (b) proposed Eq. (24), and (c) difference ratio ($T_{c-mathematical}/T_{c-FEM} - 1$)

those from FE analysis is minimal due to the small mass ratio of the secondary systems. However, as the number of secondary systems and, consequently, the mass ratio (γ) increases, the results from the two methods begin to diverge. This trend can be analyzed from two perspectives. First, as seen in all diagrams, the difference ratios for the proposed relationship are negative. This means the approximate proposed relationship consistently yields values lower than the actual ones, providing a safety margin in calculations. Second, in conventional building structures, the mass ratio of all secondary systems to the primary system is typically low, usually less than one and

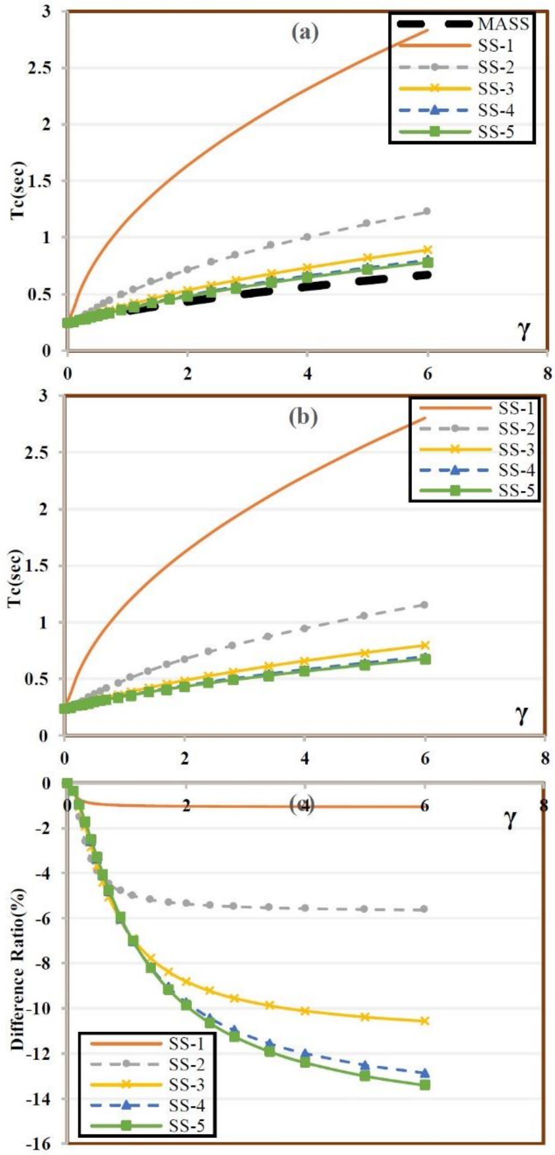

Fig. 8 Changes in time periods of one-story frame coupled with twenty secondary system against mass ratio (γ): (a) FEM, (b) proposed Eq. (24), and (c) difference ratio ($T_{c-mathematical}/T_{c-FEM} - 1$)

often less than 0.5. Despite this, the difference in period between the proposed relationship and the numerical study is less than 5%, which is generally acceptable.

It is worth mentioning that in some diagrams, the value of γ exceeds one. This occurs because the mass of the secondary system was set to be at most 30% of the story mass during selection. To better compare the effect of multiple secondary systems on the period of coupled systems, it is important to note that current seismic codes maintain a constant mass ratio for each secondary system as the number of secondary systems increases. Assuming independence between primary and secondary systems, the maximum mass of each secondary system is limited to 25% of the

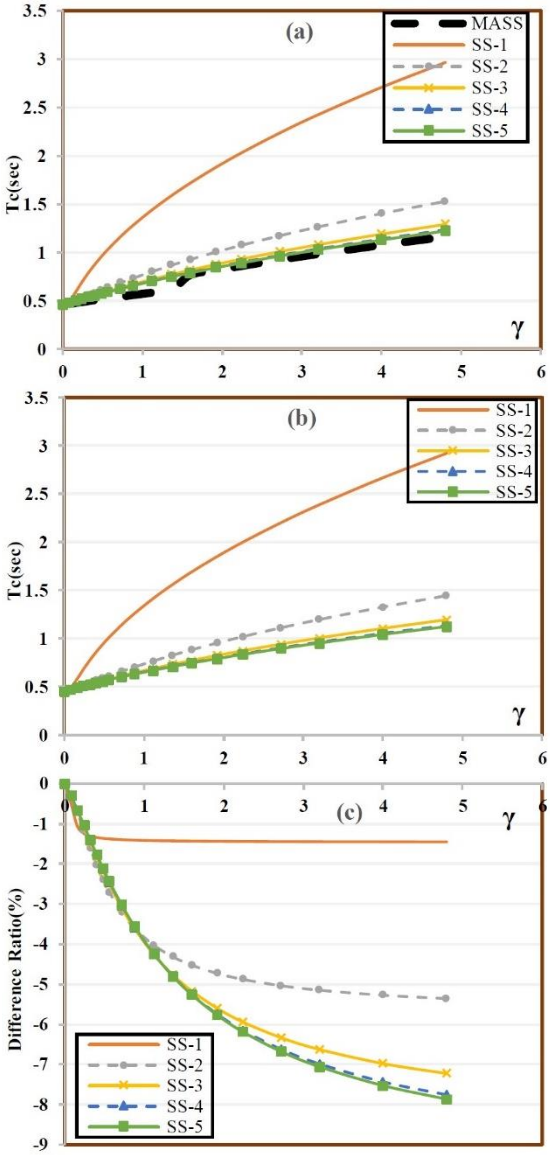

Fig. 9 Changes in time periods of two-story frame coupled with twenty secondary system against mass ratio (γ): (a) FEM, (b) proposed Eq. (24), and (c) difference ratio ($T_{c-mathematical}/T_{c-FEM} - 1$)

primary structure's mass. Therefore, if each individual secondary system meets this limit, no additional measures are necessary, even if the total number of secondary systems exceeds this limit. However, the findings of this study confirm that the multiplicity of secondary systems significantly influences the fundamental period of the coupled system when the interactions between primary and secondary systems are considered.

Based on the findings for the fundamental period of coupled frame structures with two degrees of freedom (two stories), it was found that the trend of system period variation with different mass ratios mirrors that of single degree of freedom systems. To illustrate this, a two-story frame

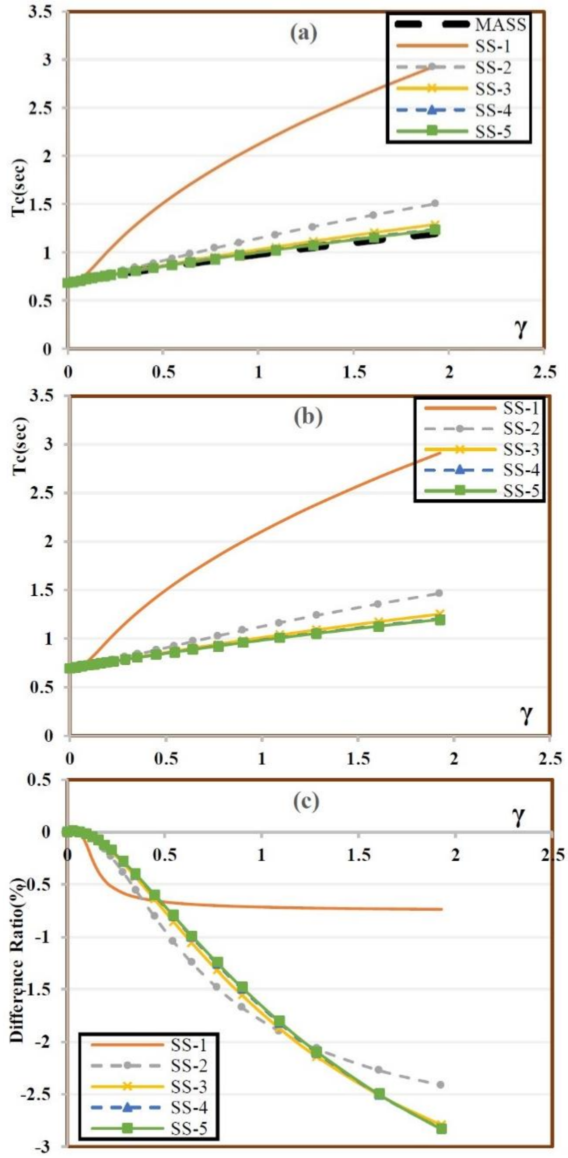

Fig. 10 Changes in time periods of three-story frame coupled with ten secondary system against mass ratio (γ): (a) FEM, (b) proposed Eq. (24), and (c) difference ratio ($T_{c-mathematical}/T_{c-FEM} - 1$)

example is provided. Fig. 9 shows the fundamental period of a two-story frame coupled with twenty secondary systems, all located on the second floor, across various mass ratios (γ). The longest system period corresponds to the secondary system with the lowest stiffness (SS1). Thus, as the stiffness of the secondary system increases, the coupled system period decreases in both analysis methods. The difference in system period between the two methods is smallest when the secondary system stiffness is lowest. However, when all secondary systems are on the first floor, a greater discrepancy between the two methods is noted, although the difference remains under 10%.

The same principles apply to frame structures with three stories. Therefore, it is seen that the

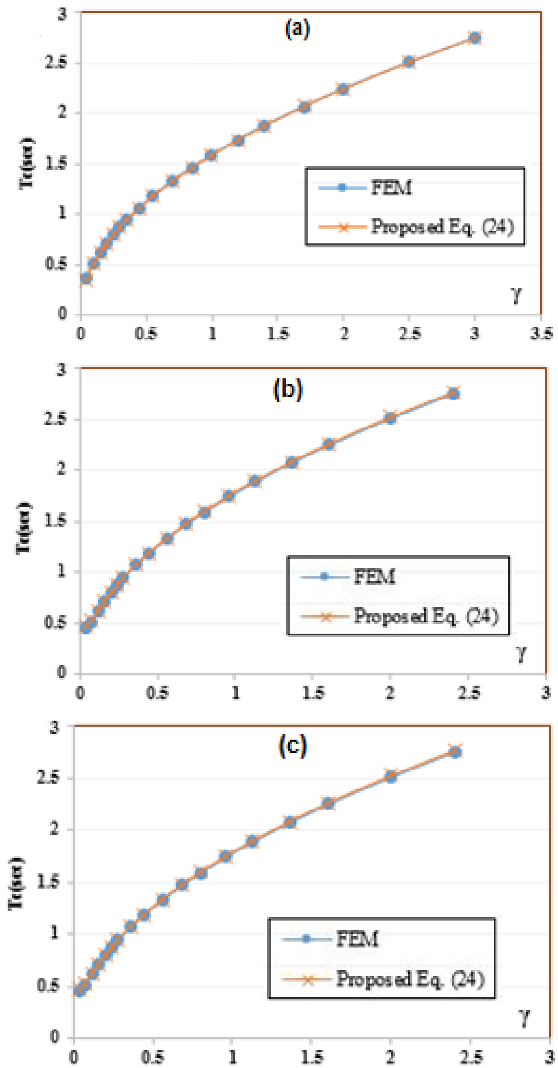

Fig. 11 Verification of FEM and mathematical approaches for time period in (a) one-story; (b) two-story; and (c) three-story coupled systems

trend of system period variation with different mass ratios is similar to that of single degree of freedom systems. An example of a three-story frame is examined below. According to Fig. 10, the fundamental period of a three-story frame coupled with ten secondary systems across various mass ratios (γ) is determined. Primarily, the longest system period is associated with the secondary system having the lowest stiffness. Hence, as the stiffness of the secondary system increases, the coupled system period decreases in both analysis methods. Furthermore, the difference in system period between the two methods is smallest when the secondary system stiffness is lowest.

In addition, Fig. 11 shows verification of FEM and mathematical approaches for time period of coupled systems for one-, two-, and three-story frames. In all figures, part (a) shows the period of the coupled system based on FEM and modal analysis of the structures, as well as time periods

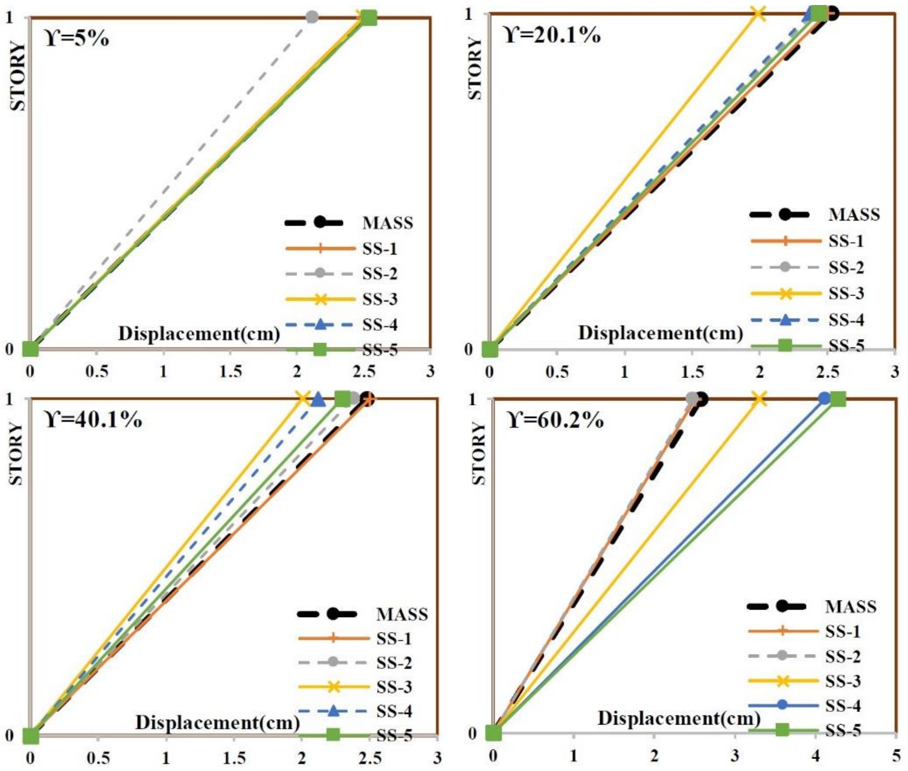

Fig. 12 Drifts versus different mass ratios for one-story coupled system

obtained from Eq. (24). In addition, part (b) also shows the differences between Eq. (24) and FEM results. Examination of these graphs clearly shows that the proposed Eq. (24) is fully efficient to be used as a design technique with a very low error and within a suitable margin of confidence. On the other hand, its simplicity and practicality can lead to its widespread use in seismic codes, which can largely compensate for the errors resulting from the lack of modeling of secondary systems.

Subsequently, the next parameter to investigate, addressing the seismic behavior of coupled systems is the relative displacement of floors in coupled systems against various mass ratios for different states of secondary systems.

Examining the diagrams of story drifts reveals that the presence or absence of the secondary system does not directly affect the relative displacement of the floors. Thus, the contribution of the secondary system, whether single or multiple at regular or irregular locations, is the effect of its period on the main period of the coupled system. As a conclusion, the overall examination of the structures with three degrees of freedom also indicates that the proposed relationship has an acceptable accuracy to be used as a design technique by engineers and practitioners. This relation (Eq. (24)) is able to predict the period of the coupled system with an acceptable accuracy when the secondary systems are distributed over all floors. In addition to the fact that the error of the proposed equation in this study is still less than 5% in the range of actual measures of mass ratios (γ) in conventional structures (which are less than 0.5), the errors are generally come in line with safety factor, demonstrating the feasibility of the proposed relation. Moreover, the investigation of

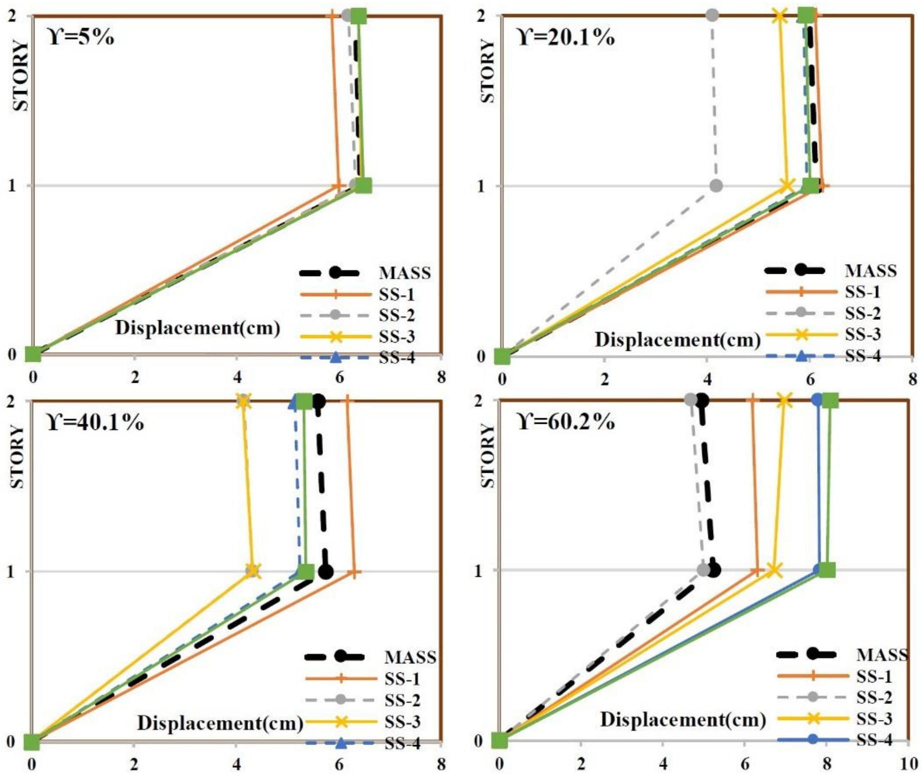

Fig. 13 Drifts versus different mass ratios for two-story coupled system

the diagrams of different structures shows that with increasing the degree of freedom of the primary structure, the amount of the mentioned error in similar situations decreases, which can be due to the better distribution of masses in the height. Another important point to note is that, at equal mass measures, the more the period of the secondary system increases compared to other secondary systems, the more the computation error increases. Also, the analysis of the diagrams shows that the main parameter in variations of the period of the primary system is the period of the secondary system. Thus, as long as the period of the secondary system is less than that of the primary system, the effects of the secondary system period can be ignored. Finally, using the coupled system period instead of the primary system period can widely reduce seismic design errors rising from ignoring secondary systems. It may also be possible to increase the period of short-period structures under the effect of the secondary system period via periodic and mass potential of secondary systems, thereby improving their seismic behavior.

5. Comparison of proposed mathematical formulation with current codes and models

As mentioned earlier, PSSI is a crucial parameter in the analysis of secondary systems. Two main approaches can be used to analyze secondary systems: (i) methods that ignore PSSI and (ii) methods that account for interaction effects. In the first approach, the primary system is analyzed

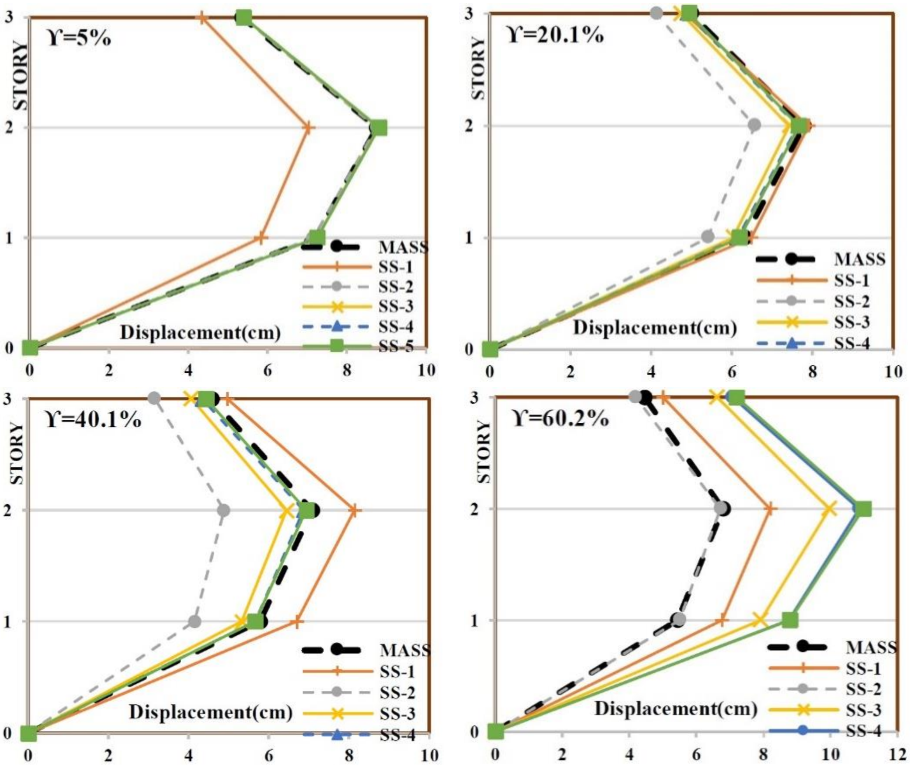

Fig. 14 Drifts versus different mass ratios for three-story coupled system

independently of the secondary system, and the acceleration response of the structure is determined at the secondary system's supports. The secondary system's response is then calculated based on the structural response at these supports. In the second approach, to account for PSSI, both primary and secondary systems must be modeled together as a single composite system, as their interaction influences the dynamic properties and responses of both systems. If the secondary system has a SDOF, the possibility of tuning must be considered. For secondary systems with MDOF or multiple supports, the correlation between support motions must be taken into account.

The initial model proposed by Singh (1980) did not account for interaction effects, leading to more conservative response estimates. Additionally, when the frequency ratio of the two systems is close to 1 and the secondary-to-primary system mass ratio is large, the estimation errors in frequency and system response increase, as reported by Gupta and Tembullkar (1984). According to Rayleigh's quotient hypothesis, a first-order error in the mode shape results in a second-order error in the frequency. Therefore, the assumptions in the model presented by Sackman *et al.* (1983a, b) led to small errors in frequency estimation. To address this limitation, Chen and Soong (1988) proposed a model based on NEHRP (1995) recommendations. Villaverde (1986a, b, 1987, 1991, 1997) suggested several simplified relations for analyzing secondary systems. However, the method by Ghafouri and Fiouz (2004) for calculating the response of secondary systems has a flaw: if the connection of the secondary system to the primary structure is highly flexible, the frequency of the secondary system tends to zero, leading to zero acceleration without any applied force, which is impractical. Based on this issue, the relations presented in IBC (2006) have several fundamental drawbacks: (i) the recommended equivalent static force is not correlated with the dynamic characteristics of the primary structure, (ii) changes in the equivalent static force are assumed to be linear with the height of the structure, and (iii) the determination of the intensity coefficient, which indicates the degree of flexibility of the secondary system, lacks sufficient accuracy.

In addition to the previously discussed models, Biggs and Roesset (1970, 1972) and Sackman and Kelly (1978, 1979) proposed a widely used method in practice. However, this method has several significant limitations: (i) it is only suitable for secondary systems with natural frequencies that differ greatly from those of the primary structure and where the secondary system mass is small compared to the primary structure, (ii) it produces unrealistic results for secondary systems with multiple supports. According to UBC (1997), the force acting on nonstructural elements is calculated based on ultimate strength, while the magnification factor of the secondary system can be determined using the dynamic properties of both the structure and the secondary element. Additionally, ASCE7-10 (2010) reduced the magnification factor related to the location of the nonstructural element from 0.3 to 0.2. According to New Zealand's NZS4219 (2004, 2009) requirements, the seismic load on secondary systems is estimated using the static equivalent force. Furthermore, the relationship proposed in Eurocode (2008) calculates the horizontal earthquake force based on the ultimate strength at the center of mass of the secondary system in the direction of greatest effect.

Most codes and standards for seismic calculations and responses of secondary systems rely on estimating equivalent seismic lateral forces, which are directly proportional to the weight of the secondary system. However, for secondary systems with multiple supports, these codes lack specific relationships or seismic conditions and only propose displacement control of the supports. This oversight is due to the complexity of interactions between primary and secondary systems, leading to the neglect of Primary-Secondary System Interaction (PSSI) in current methods and standards. As a result, the calculation and design of these systems are treated independently. Furthermore, existing codes and standards do not account for the location of the secondary system at the roof level. The relationships proposed in this study aim to address the limitations of current seismic design methods.

6. Conclusions

This study conducted a FE and mathematical investigation to estimate the time period of coupled primary-secondary structural systems. To this end, several three-dimensional (3D) steel moment-resisting frame structures with one, two, and three stories, each featuring four perimeter columns and four perimeter beams per story, were modeled using a FE software, as primary systems. The goal was to evaluate the impacts of secondary system multiplicity, their distribution across different stories, and the number of stories (degrees of freedom) on the period of the coupled structure. Key findings from the study include:

- Even with very low mass, the addition of secondary systems to the primary structure significantly alters the period of the coupled system.
- The most notable impact of the secondary system on the coupled system's response is on the structural period during the design process.
- The proposed approach allows for modifying the period of primary structures to lower values,

enabling the coupled structure to benefit from increased period values by leveraging multiple secondary systems.

• The fundamental period of a one-story frame structure coupled with one secondary system increases with a higher mass ratio (γ) in both numerical and analytical approaches. This trend is also observed in systems with higher degrees of freedom.

• Increasing the stiffness of the secondary system reduces the period of the coupled primary-secondary structure.

• The ratio of the periodic difference ($T_{c-mathematical}/T_{c-FEM} - 1$) generally increases with a higher mass ratio (γ). This discrepancy is smallest when the secondary system has the lowest stiffness and increases as the secondary system stiffness escalates.

• The difference between the results from the proposed relationship and numerical analysis is minimal due to the small mass ratio of the secondary systems. However, the results begin to diverge as the number of secondary systems increases.

• If the period of the secondary system is less than that of the primary system, the effects of the secondary system period can be ignored.

References

Adam, C. (2001), “Dynamics of elastic-plastic shear frames with secondary structures: Shake table and numerical studies”, *Earthq. Eng. Struct. Dyn.*, **30**(2), 257-277. https://doi.org/10.1002/1096-9845(200102)30:2<257::AID-EQE7>3.0.CO;2-J.

Alami, F. and Khotimah, S.N. (2017), Manual Structural Analysis Program (SAP) 2000.

ASCE Standard ASCE/SEI 7-10 (2010), Minimum Design Load for Buildings and Other Structures, American Society of Civil Engineering Standard, Reston, Virginia.

Asteris, P.G., Repapis, C.C., Foskolos, F., Fotos, A. and Tsaris, A.K. (2017), “Fundamental period of infilled RC frame structures with vertical irregularity”, *Struct. Eng. Mech.*, **61**(5), 663-674. https://doi.org/10.12989/sem.2017.61.5.663.

Biggs, J.M. (1972), “Seismic response spectra for equipment design in nuclear power plants”, No. EUR-4820, V. 5, PT. K.

Biggs, J.M. and Roesset, J.M. (1970), “Seismic analysis of equipment mounted on a massive structure”, Massachusetts Inst. of Tech., Cambridge.

Butenweg, C., Bursi, O.S., Nardin, C., Lanese, I., Pavese, A., Marinković, M., Paolacci, F. and Quinci, G. (2021), “Experimental investigation on the seismic performance of a multi-component system for major-hazard industrial facilities”, *Press. Ves. Pip. Conf.*, **85352**, V005T08A016. https://doi.org/10.1115/PVP2021-61696.

Butenweg, C., Bursi, O.S., Paolacci, F., Marinković, M., Lanese, I., Nardin, C. and Quinci, G. (2021), “Seismic performance of an industrial multi-storey frame structure with process equipment subjected to shake table testing”, *Eng. Struct.*, **243**, 112681. https://doi.org/10.1016/j.engstruct.2021.112681.

Caicedo, D., Lara-Valencia, L., Blandon, J. and Graciano, C. (2021), “Seismic response of high-rise buildings through metaheuristic-based optimization using tuned mass dampers and tuned mass dampers inerter”, *J. Build. Eng.*, **34**, 101927. https://doi.org/10.1016/j.jobe.2020.101927.

Chalarca, B., Filiatrault, A. and Perrone, D. (2020), “Seismic demand on acceleration-sensitive nonstructural components in viscously damped braced frames”, *J. Struct. Eng.*, **146**(9), 4020190. https://doi.org/10.1061/(ASCE)ST.1943-541X.0002770.

Charalampakis, A.E., Tsiatas, G.C. and Kotsiantis, S.B. (2020), “Machine learning and nonlinear models for the estimation of fundamental period of vibration of masonry infilled RC frame structures”, *Eng. Struct.*, **216**, 110765. https://doi.org/10.1016/j.engstruct.2020.110765.

Chen, Y. and Soong, T.T. (1988), “Seismic response of secondary systems”, *Eng. Struct.*, **10**(4), 218-228.

https://doi.org/10.1016/0141-0296(88)90043-0.
De, M., Sengupta, P. and Chakraborty, S. (2018), "Fundamental periods of reinforced concrete building frames resting on sloping ground", *Earthq. Struct.*, **14**(4), 305-312. https://doi.org/10.12989/eas.2018.14.4.305.
Dhakal, R.P., Pourali, A., Tasligedik, A.S., Yeow, T., Baird, A., MacRae, G., Pampanin, S. and Palermo, A. (2016), "Seismic performance of non-structural components and contents in buildings: an overview of NZ research", *Earthq. Eng. Eng. Vib.*, **15**, 1-17. https://doi.org/10.1007/s11803-016-0301-9.
Filiatrault, A., Perrone, D., Merino, R.J. and Calvi, G.M. (2021), "Performance-based seismic design of nonstructural building elements", *J. Earthq. Eng.*, **25**(2), 237-269. https://doi.org/10.1080/13632469.2018.1512910.
Ghafoori-Ashtiani, M. and Foyooz, A. (2022), "Absolute acceleration transfer function of secondary systems subjected to multi-component earthquakes", *J. Adv. Mater. Eng. (Esteghlal)*, **21**(1), 113-139.
Ghafouri, A.M. and Fiouz, A.R. (2004), "Response of secondary systems subjected to multicomponent earthquake input", *J. Seismol. Earthq. Eng.*, **6**(2), 29-45.
Gupta, A.K. and Tembulkar, J.M. (1984), "Dynamic decoupling of secondary systems", *Nucl. Eng. Des.*, **81**(3), 359-373. https://doi.org/10.1016/0029-5493(84)90282-6.
Jiang, R., Jiang, L., Hu, Y., Jiang, L. and Ye, J. (2020a), "A simplified method for fundamental period prediction of steel frames with steel plate shear walls", *Struct. Des. Tall Spec. Build.*, **29**(7), e1718. https://doi.org/10.1002/tal.1718.
Jiang, R., Jiang, L., Hu, Y., Ye, J. and Zhou, L. (2020b), "A simplified method for estimating the fundamental period of masonry infilled reinforced concrete frames", *Struct. Eng. Mech.*, **74**(6), 821-832. https://doi.org/10.12989/sem.2020.74.6.821.
Kazantzi, A.K., Miranda, E. and Vamvatsikos, D. (2020), "Strength-reduction factors for the design of light nonstructural elements in buildings", *Earthq. Eng. Struct. Dyn.*, **49**(13), 1329-1343. https://doi.org/10.1002/eqe.3292.
Lahdiri, A. and Kadri, M. (2024), "Isogeometric analysis of the seismic response of a gravity dam: A comparison with FEM", *Adv. Comput. Des.*, **9**(2), 81-96. https://doi.org/10.12989/acd.2024.9.2.081.
Merino, R.J., Perrone, D. and Filiatrault, A. (2019), "Consistent floor response spectra for performance-based seismic design of nonstructural elements", *J. Earthq. Eng. Struct. Dyn.*, **49**(3), 261-284. https://doi.org/10.1002/eqe.3236.
Moeindarbari, H. and Taghikhany, T. (2014), "Seismic optimum design of triple friction pendulum bearing subjected to near-fault pulse-like ground motions", *Struct. Multidisc. Optim.*, **50**, 701-716. https://doi.org/10.1007/s00158-014-1079-x.
NZS1170.5 (2004), Structural Design Actions Part 5: Earthquake Action, Standard New Zealand.
NZS4219 (2009), Seismic Performance of Engineering Systems in Buildings, Standard New Zealand.
Pandian, A.V.P. and Vinu, M. (2023), Effects of Fundamental Natural Time Periods on the Seismic Performance of Base Isolated Multistory Buildings.
Perrone, D., Calvi, P.M., Nascimbene, R., Fischer, E.C. and Magliulo, G. (2019), "Seismic performance of non-structural elements during the 2016 Central Italy earthquake", *Bull. Earthq. Eng.*, **17**, 5655-5677. https://doi.org/10.1007/s10518-018-0361-5.
Ryan, K.L., Soroushian, S., Maragakis, E.M., Sato, E., Sasaki, T. and Okazaki, T. (2016), "Seismic simulation of an integrated ceiling-partition wall-piping system at E-Defense. I: Three-dimensional structural response and base isolation", *J. Struct. Eng.*, **142**(2), 04015130. https://doi.org/10.1061/(ASCE)ST.1943-541X.0001384.
Sackman, J.L. and Kelly, J.M. (1978), "Rational design methods for light equipment in structures subjected to ground motion", NASA STI/Recon Technical Report No, 79, 25259.
Sackman, J.L. and Kelly, J.M. (1979), "Seismic analysis of internal equipment and components in structures", *Eng. Struct.*, **1**(4), 179-190. https://doi.org/10.1016/0141-0296(79)90045-2.
Sackman, J.L., Der Kiureghian, A. and Nour-Omid, B. (1983), "Dynamic analysis of light equipment in structures: modal properties of the combined system", *J. Eng. Mech.*, **109**(1), 73-89. https://doi.org/10.1061/(ASCE)0733-9399(1983)109:1(73).

Sari, A. and Korkmaz, K. (2024), "An analytical approach for offshore structures considering soil-structure interaction", *Adv. Comput. Des.*, **9**(1), 25-38. https://doi.org/10.12989/acd.2024.9.1.025.

Singh, M.P. (1980), "Seismic design input for secondary systems", *J. Struct. Div.*, **106**(2), 505-517. https://doi.org/10.1061/JSDEAG.0005371.

Standard, B. (2005), Eurocode 8: Design of Structures for Earthquake Resistance, Part, 1, 1998-1.

Surana, M. (2019), "Evaluation of seismic design provisions for acceleration-sensitive non-structural components", *Earthq. Struct.*, **16**(5), 611-623. https://doi.org/10.12989/eas.2019.16.5.611.

Uniform Building Code (1997), Chapter 16: Section 1632-Lateral Force on Elements of Structures, Non-Structural Components and Equipment Supported by Structures, U.S.A.

Villaverde, R. (1986a), "Simplified seismic analysis of secondary systems", *J. Struct. Eng.*, **112**(3), 588-604. https://doi.org/10.1061/(ASCE)0733-9445(1986)112:3(588).

Villaverde, R. (1986b), "Simplified seismic analysis of piping or equipment mounted on two points of a multistory structure", *Nucl. Eng. Des.*, **92**(1), 37-50. https://doi.org/10.1016/0029-5493(86)90097-X.

Villaverde, R. (1987), "Simplified approach for the seismic analysis of equipment attached to elastoplastic structures", *Nucl. Eng. Des.*, **103**(3), 267-279. https://doi.org/10.1016/0029-5493(87)90310-4.

Villaverde, R. (1991), "Approximate formulas to calculate the seismic response of light attachments to buildings", *Nucl. Eng. Des.*, **128**(3), 349-368. https://doi.org/10.1016/0029-5493(91)90172-E.

Villaverde, R. (1997), "Seismic design of secondary structures: State of the art", *J. Struct. Eng.*, **123**(8), 1011-1019. https://doi.org/10.1061/(ASCE)0733-9445(1997)123:8(1011).

Yang, T.Y., Qiao, T., Tobber, L. and Rodgers, G.W. (2022), "Seismic performance of controlled outrigger rocking wall system with different energy dissipation devices", *Soil Dyn. Earthq. Eng.*, **155**, 107179. https://doi.org/10.1016/j.soildyn.2022.107179.

Zhang, D., Peng, X. and Zhang, D. (2024), "Simulating flow-induced fiber motion with finite element based explicit coupling method", *Adv. Comput. Des.*, **9**(3), 229-252. https://doi.org/10.12989/acd.2024.9.3.229.

Zhao, Q., Qiu, J., Zhao, Y. and Yu, C. (2020), "Estimating fundamental period of corrugated steel plate shear walls", *KSCE J. Civil Eng.*, **24**, 3023-3033. https://doi.org/10.1007/s12205-020-2305-2.

List of symbols and acronyms

PSSI	: primary-secondary system interactions
MDOF	: multi degrees-of-freedom
MRF	: moment-resisting frame
i Index	: degree of freedom of the primary system
j Index	: degree of freedom of the secondary system
SDOF	: single degree-of-freedom
$m_{s\,ij}$	: mass of the j-th secondary system, connected to i-th degree of freedom in the primary system
$k_{s\,ij}$	: stiffness of the j-th secondary system, connected to i-th degree of freedom in the primary system
$[M_p]$	: mass matrix of the primary system
$[K_p]$	: stiffness matrix of the primary system
$[M_c]$	: mass matrix of the coupled system
$[K_c]$	: stiffness matrix of the coupled system
$\{\varphi_r{}^*\}$	: modal vector in shape mode r
$\{k_s\varphi^*\}$	: vector for secondary systems effect on primary system

M_1	: primary system mass contributing to the first mode
T_p	: primary system time period
T_{se}	: secondary system effective time period
T_c	: coupled system time period
ω_p	: frequency of the first mode of the primary system
ω_c	: frequency of the first mode of the coupled system
ω_{se}	: effective frequency of the secondary systems
F_T	: ratio of coupled system period to primary system period
f_T	: ratio of secondary system period to primary system period
R_F	: ratio of coupled system frequency to primary system frequency
r_F	: ratio of secondary system frequency to primary system frequency
γ	: mass ratio
$T_{c-mathematical}$	: fundamental period obtained via mathematical approach
$T_{c-\mathrm{FEM}}$	: fundamental period obtained via FEM approach
w_p	: primary system story weight
w_{sr}	: r-th secondary system weight
3D	: three-dimensional
SAP	: structural analysis program
PEER-NGA	: pacific earthquake engineering research
ASCE	: American society of civil engineering
PGA	: peak ground acceleration
PGV	: peak ground velocity
SLE	: service level earthquake
DBE	: design basis earthquake
MCE	: maximum considered earthquake
CDP	: concrete damage plasticity
SS	: Secondary system